CHEMISTRY OF MATERIALS

Article

pubs.acs.org/cm

Thermal Atomic Layer Etching of Titanium Nitride Using Sequential, Self-Limiting Reactions: Oxidation to TiO_2 and Fluorination to Volatile TiF_4

Younghee Lee[†] and Steven M. George*[,†,‡]

[†]Department of Chemistry and Biochemistry, University of Colorado, Boulder, Colorado 80309, United States

[‡]Department of Mechanical Engineering, University of Colorado, Boulder, Colorado 80309, United States

ABSTRACT: The thermal atomic layer etching (ALE) of TiN was demonstrated using a new etching mechanism based on sequential, self-limiting oxidation and fluorination reactions. The oxidation reactant was either O_3 or H_2O_2, and the fluorination reactant was hydrogen fluoride (HF) derived from HF-pyridine. In the proposed reaction mechanism, the O_3 reaction oxidizes the surface of the TiN substrate to a TiO_2 layer and gaseous NO. HF exposure to the TiO_2 layer then produces TiF_4 and H_2O as volatile reaction products. The overall reaction can be written as $TiN + 3O_3 + 4HF \rightarrow TiF_4 + 3O_2 + NO + 2H_2O$. Quartz crystal microbalance studies showed that HF can spontaneously etch TiO_2 films. Spectroscopic ellipsometry and X-ray reflectivity analysis showed that TiN films were etched linearly versus the number of ALE cycles using O_3 and HF as the reactants. The TiN etching also occurred selectively in the presence of Al_2O_3, HfO_2, ZrO_2, SiO_2, and Si_3N_4. The etch rate for TiN ALE was determined at temperatures from 150 to 350 °C. The etch rates increased with temperature from 0.06 Å/cycle at 150 °C to 0.20 Å/cycle at 250 °C and stayed nearly constant for temperatures ≥250 °C. TiN ALE was also accomplished using H_2O_2 and HF as the reactants. The etch rate was 0.15 Å/cycle at 250 °C. The TiN films were smoothed by TiN ALE using either the O_3 or H_2O_2 oxidation reactants. The thermal ALE of many other metal nitrides should be possible using this new etching mechanism based on oxidation and fluorination reactions. This thermal ALE mechanism should also be applicable to metal carbides, metal sulfides, metal selenides, and elemental metals that have volatile metal fluorides.

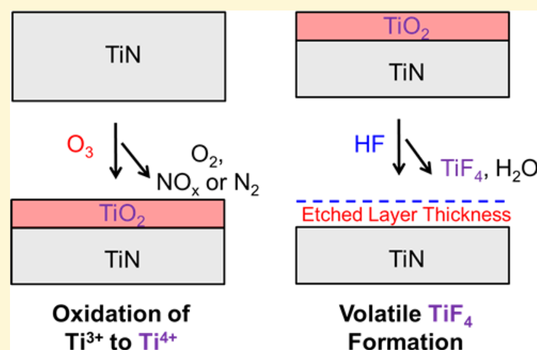

I. INTRODUCTION

Atomic layer etching (ALE) is a thin-film removal method based on sequential, self-limiting surface reactions.[1,2] ALE is usually defined by two separate reactions that enable atomic-level removal of thin films. The ALE process is the reverse of atomic layer deposition (ALD).[3,4] The first reaction during ALE is often an activation step where the surface of the film is modified by adsorption of a reactive species. The second reaction is then the removal of this activated layer using high-energy collisions.[1,5] Energetic ions or noble gas atoms have been used to remove the activated material in many previously reported ALE processes.[1,6]

Thermal ALE processes have also been developed recently using sequential, self-limiting fluorination and ligand-exchange reactions.[7,8] For metal oxide ALE, a gas-phase fluorination reagent, such as HF, forms a stable and nonvolatile fluoride layer on the metal oxide film. Metal reagents then can remove the fluoride layer through ligand-exchange transmetalation reactions.[9] Thermal ALE processes for Al_2O_3, HfO_2, ZrO_2, ZnO, SiO_2, AlN, and AlF_3 have been demonstrated using HF and various metal precursors such as $Sn(acac)_2$, trimethylaluminum, dimethylaluminum chloride, and silicon tetrachloride.[7,8,10−18]

The thermal ALE process using fluorination and ligand-exchange reactions has not been able to etch some metal nitrides, such as titanium nitride (TiN).[15] TiN is an important material as a copper diffusion barrier and a complementary metal−oxide−semiconductor (CMOS) gate electrode material in semiconductor devices.[19,20] Previous thermal ALE studies have observed that TiN was not etched using HF together with a variety of metal precursors for ligand-exchange.[15] One reason for observing no etching is that the oxidation state of Ti in TiN is 3+. Fluorination would retain the oxidation state by fluorinating TiN to TiF_3. However, the oxidation state of Ti is 4+ for most stable and volatile Ti compounds. The ligand-exchange process for TiF_3 does not produce a stable and volatile reaction product.[15]

Different approaches are needed for thermal TiN ALE. A new thermal ALE process can be defined by sequential, self-limiting oxidation and fluorination reactions as illustrated in Figure 1. The first step is the oxidation reaction where an ozone (O_3) exposure produces a titanium oxide (TiO_2) surface layer on the TiN substrate:

Received: June 2, 2017
Revised: August 22, 2017
Published: September 12, 2017

 © 2017 American Chemical Society

DOI: 10.1021/acs.chemmater.7b02286
Chem. Mater. 2017, 29, 8202−8210

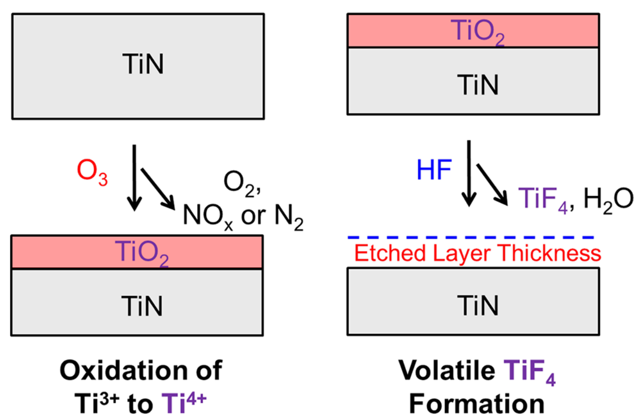

Figure 1. Schematic for TiN ALE using O_3 and HF as the reactants. O_3 oxidizes the TiN substrate to form a TiO_2 layer on the surface. Subsequently, HF removes the TiO_2 layer by forming volatile TiF_4 and H_2O reaction products.

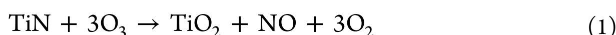

$$TiN + 3O_3 \rightarrow TiO_2 + NO + 3O_2 \quad (1)$$

O_3 is a strong oxidant that is able to convert the oxidation state of Ti from 3+ to 4+. This oxidation reaction is thermochemically favorable.[21] O_3 can also form a stable, self-passivating TiO_2 layer. The TiO_2 layer forms a diffusion barrier that impedes further oxidation and leads to a self-limiting oxidation reaction.

A fluorinating reagent, such as HF, can then react with TiO_2 and form a volatile titanium tetrafluoride (TiF_4) reaction product:

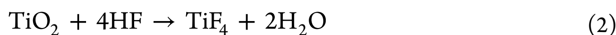

$$TiO_2 + 4HF \rightarrow TiF_4 + 2H_2O \quad (2)$$

This fluorination reaction is thermochemically favorable at room temperature and becomes less favorable at higher temperatures.[21] The TiF_4 reaction product will be removed from the surface because of its high volatility. H_2O is also produced as a volatile reaction product. The O_3 and HF reactions can then be repeated to etch the TiN substrate with atomic layer control.

The thermal ALE process shown in Figure 1 using oxidation and fluorination reactions is very different from the previous thermal ALE approach using fluorination and ligand-exchange reactions. In the new process illustrated in Figure 1, HF etches the TiO_2 layer by producing volatile TiF_4. In contrast, the fluorination step in the previous thermal ALE approach has been used to form stable and nonvolatile metal fluorides such as AlF_3, ZrF_4, and HfF_4.[8,11,13,15] These stable metal fluorides were then removed by a ligand-exchange reaction.

This new thermal ALE process should be valuable for a number of conducting transition metal nitrides such as TiN, VN, TaN, and WN. These metal nitrides have an oxidation state of 3+ that is lower than the oxidation state in their fully oxidized forms. The fluorides of these metal nitrides may have difficulty undergoing ligand-exchange reactions. However, oxidation can convert these metal nitrides to metal oxides with higher oxidation states. For example, the TiO_2, V_2O_5, Ta_2O_5, and WO_3 metal oxides have oxidation states of 4+, 5+, 5+, and 6+, respectively. The TiF_4, VF_5, TaF_5, and WF_6 metal fluorides that may form during the fluorination of these metal oxides have high volatility and share the same high oxidation states as their respective metal oxides.

In this work, thermal TiN ALE was demonstrated using oxidation and fluorination reactions. O_3 or H_2O_2 vapor was employed as the oxidation reactant. HF vapor derived from HF-pyridine solution was used as the fluorination reactant. Spectroscopic ellipsometry was used to measure the thicknesses of TiN thin films on silicon wafers versus the number of ALE cycles. X-ray reflectivity measurement was also employed to confirm the thickness changes as well as to determine the roughness of the TiN film after ALE reactions.

The oxidation and fluorination reactions were also used to demonstrate the selective etching of TiN in the presence of other materials such as Al_2O_3, HfO_2, ZrO_2, SiO_2, and Si_3N_4. These materials are all important materials in semiconductor fabrication processes. This thermal ALE strategy using oxidation and fluorination reactions that yield a volatile metal fluoride is general and should provide a pathway for the thermal ALE of a number of new materials. In addition to other metal nitrides, possible new materials include metal carbides, metal sulfides, metal selenides, and elemental metals.

II. EXPERIMENTAL SECTION

All the reactions were conducted in a viscous-flow, hot-wall reactor defined by a stainless steel tube with the length of ~60 cm and inside diameter of 3.8 cm.[22] The reactor was isothermally heated by heating elements attached to the outside of the stainless steel tube. The reaction temperatures from 150 to 350 °C were stabilized within ±0.04 °C of the set point by a proportional-integral-derivative (PID) temperature controller (2604, Eurotherm). A constant flow of 150 sccm UHP nitrogen gas (N_2, 99.999%, Airgas) was regulated by mass flow controllers (Type 1179A, MKS). This N_2 gas flow established a base pressure of ~1 Torr in the reactor when pumped by a mechanical pump (Pascal 2015SD, Alcatel). The pressure was recorded by a capacitance manometer (Baratron 121A, MKS).

The demonstration of spontaneous etching of TiO_2 was performed using an *in situ* quartz crystal microbalance (QCM) located at the center of the hot-wall reactor.[22] The gold-coated quartz crystal (polished, RC crystal, 6 MHz, Phillip Technologies) was placed in a sensor head (BSH-150, Inficon) and sealed with high-temperature epoxy (Epo-Tek H21D, Epoxy Technology). The mass changes during the reactions were measured by a thin-film deposition monitor (Maxtek TM-400, Inficon). The TiO_2 films were deposited on the QCM crystal using TiO_2 ALD with titanium tetrachloride ($TiCl_4$, 99%, Strem) and deionized H_2O (Chromasolv for HPLC, Sigma-Aldrich) as the reactants at 200, 250, and 300 °C.[23] HF exposures on these TiO_2 ALD films were performed at the same temperature as the TiO_2 ALD reactions.

The HF source was a HF-pyridine solution (70 wt % HF, Sigma-Aldrich). A gold-plated stainless steel bubbler was filled with the HF-pyridine solution in a dry N_2-filled glovebag and held at room temperature. A HF vapor pressure of 90−100 Torr was in equilibrium with the HF-pyridine solution.[11] Only HF vapor was delivered in the gas phase as confirmed by mass spectrometry.[24] The pressure transients of HF were adjusted to ~80 mTorr using a metering bellows-sealed valve (SS-4BMG, Swagelok).

The O_3 was produced in a corona discharge ozone generator (LG-14, Del Ozone). A flow of 480 sccm of UHP oxygen gas (O_2, 99.994%, Airgas) was supplied to produce a maximum ~5 wt % of O_3 in O_2. When the O_3 was not delivered to the reactor, the O_3 was passed through an ozone destruct unit (ODS-1, Ozone Solutions) connected to the exhaust line. Hydrogen peroxide (H_2O_2) vapor was evaporated with H_2O from a H_2O_2 solution (50 wt %, Sigma-Aldrich) contained in a glass bubbler. The H_2O_2 solution was held at room temperature.

The TiN films were prepared by SEMATECH. The TiN film was deposited on a 300 mm diameter silicon wafer by semiconductor ALD processes in commercially available tools. The initial thickness of TiN was measured as ~70 Å by spectroscopic ellipsometry (SE) measurements. The TiN film on the silicon wafers was cleaved to produce samples that were 1.25 cm by 1.25 cm in size and used in the ALE experiments. For the selectivity experiments, the Al_2O_3, HfO_2, ZrO_2, SiO_2, and Si_3N_4 thin films on silicon wafers were placed together with the TiN sample in the reactor. The Al_2O_3, HfO_2, and ZrO_2 films

DOI: 10.1021/acs.chemmater.7b02286
Chem. Mater. 2017, 29, 8202−8210

were prepared by SEMATECH and deposited by ALD processes. The SiO_2 and Si_3N_4 films were prepared by SEMATECH and deposited by chemical vapor deposition (CVD) processes.

Al_2O_3 ALD films were coated inside the reactor before TiN ALE to minimize O_3 decomposition on the walls of the hot-wall reactor.[25] The ALE reactions were conducted using a reaction sequence represented as x-30-y-30. This reaction sequence consists of an exposure of the oxidation reagent for x s, 30 s of N_2 purge, y s of HF exposure, and 30 s of N_2 purge. The ALE reactions using O_3 as an oxidation reagent were performed using an optimized reaction sequence of 3-30-1-30. The ALE reactions using H_2O_2 as an oxidation source were performed using an optimized reaction sequence of 2.5-30-1-30.

Ex situ spectroscopic ellipsometry (SE) measurements determined the thicknesses of the various films. Ψ and Δ at 240−900 nm were measured by a spectroscopic ellipsometer (M-2000, J. A. Woollam) and fitted by the analysis software (CompleteEASE, J. A. Woollam). These measurements employed an incidence angle of 75° near the Brewster angle of the silicon wafer. A Lorentz model was used for fitting the thickness of the TiN film. A Sellmeier model was used for fitting of the Al_2O_3, HfO_2, ZrO_2, SiO_2, and Si_3N_4 films.

The thicknesses, roughness, and film density were obtained by *ex situ* XRR analysis. The X-ray reflectivity (XRR) scans at 300−9000 arcsec were measured by a high-resolution X-ray diffractometer (Bede D1, Jordan Valley Semiconductors) using Cu Kα radiation (λ = 1.540 Å). The filament voltage was 40 kV, and the current was 35 mA in the X-ray tube. All XRR scans were recorded with a 10 arcsec step size and a 5 s acquisition time and fitted using the analysis software (Bede REFS, Jordan Valley Semiconductors) to determine film thickness, film density, and surface roughness.

III. RESULTS AND DISCUSSION

A. Spontaneous Etching of TiO_2 by HF. Figure 2 shows the mass changes during 10 consecutive HF exposures on TiO_2 films grown on the quartz crystal microbalance. The TiO_2 ALD films were deposited using $TiCl_4$ and H_2O as the reactants at 200, 250, and 300 °C.[23] Each HF exposure for 1 s leads to a mass loss consistent with spontaneous etching of the TiO_2 film. The average mass change during the HF exposure is −17 ng/cm^2 at 200 °C. There are slightly higher mass changes at higher temperatures. Mass changes of −25 and −32 ng/cm^2 were obtained with the same HF exposure time of 1 s at 250 and 300 °C, respectively. These results suggest that an HF exposure of 1 s is able to etch a TiO_2 thickness of 0.66−0.85 Å at 250−300 °C based on the density of 3.76 g/cm^3 for TiO_2 ALD films.[23]

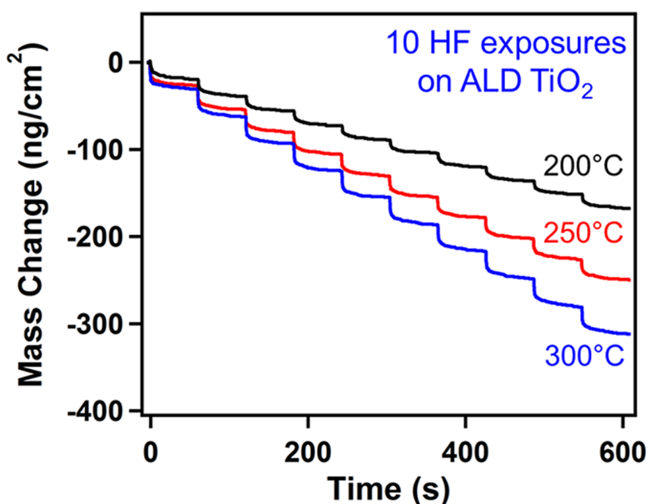

Figure 2. Mass changes during 10 consecutive HF exposures on TiO_2 ALD film at 200, 250, and 300 °C.

The fluorination reaction given by eq 2 has a standard reaction enthalpy $\Delta H°$ = −22.7 kcal/mol at 25 °C.[21] This negative enthalpy value is maintained at high temperatures with $\Delta H°$ = −21.9 kcal/mol at 250 °C.[21] The standard free energy of this reaction is favorable at room temperature with $\Delta G°$ = −6.1 kcal/mol at 25 °C.[21] The standard free energy change becomes unfavorable at temperatures >150 °C for entropic reasons. The $\Delta G°$ value at 250 °C is +6.3 kcal/mol.[21] However, the ΔG values for the HF reaction with TiO_2 may be negative and may predict a spontaneous reaction under nonstandard conditions. The etching could be favorable in the presence of excess of HF vapor when the TiF_4 and H_2O reaction products are quickly removed by the N_2 purge gas.

B. Thermal TiN ALE Using O_3 and HF. Previous studies have shown that HF by itself or in conjunction with other metal precursors cannot etch TiN.[15] However, HF is able to etch TiO_2 spontaneously as shown in Figure 2. These results suggest that if a TiO_2 layer can be formed on a TiN substrate using an oxidizing reagent, then a fluorination reagent, such as HF, should be able to etch the TiO_2 layer on the TiN substrate. These oxidation and fluorination reactions define the thermal TiN ALE process illustrated in Figure 1.

Ozone (O_3) is a gas-phase reagent with strong oxidation power. O_3 has often been preferred to O_2 as an oxygen source for metal oxide ALD when its stronger oxidizing ability is needed, or the H_2O purge is difficult.[26] In addition, O_3 is also known to form an excellent passivation oxide layer on polycrystalline aluminum metal or crystalline silicon.[27,28] O_3 also can be employed as an oxidation reagent for the formation of a TiO_2 layer on the TiN substrate.

The proposed oxidation reaction of TiN using O_3 is given by eq 1. This oxidation reaction is thermochemically favorable. The standard free energy of this reaction is $\Delta G°$ = −242.1 kcal/mol at 250 °C.[21] Other nitrogen-containing reaction products in addition to NO, such as N_2 and NO_2, may be possible. The $\Delta G°$ values with N_2 or NO_2 as the reaction product yield favorable standard free energy values of $\Delta G°$ = −219 or −288 kcal/mol at 250 °C, respectively.[21]

The fluorination reaction of HF with TiO_2 is given by eq 2. This reaction has $\Delta G°$ values of −6.1 kcal/mol at 25 °C and +6.3 kcal/mol at 250 °C.[21] As discussed above in Section A, the positive $\Delta G°$ value at 250 °C does not preclude the reaction because the reactions are not performed under standard conditions. The production of TiF_4 can lead to etching because TiF_4 is a volatile solid that sublimes at 284 °C.[29]

After HF removes the TiO_2 layer on the TiN substrate, HF could also form TiF_3 by fluorination of TiN. The reaction between TiN and HF is given by

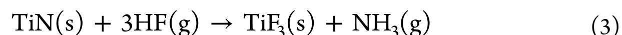

$$TiN(s) + 3HF(g) \rightarrow TiF_3(s) + NH_3(g) \quad (3)$$

This reaction is favorable with a $\Delta G°$ value of −37.0 kcal/mol at 250 °C.[21] TiF_3 is a nonvolatile solid with a melting point of 1200 °C and boiling point of 1400 °C.[29] TiF_3 may act as an etch stop. However, the HF reaction with TiN may not occur if HF does not remove the entire TiO_2 film or does not remove the TiO_xN_y layer at the interface between TiO_2 and TiN.

Figure 3 shows the spectroscopic ellipsometry (SE) and X-ray reflectivity (XRR) measurements of the initial TiN film thickness and the TiN film thickness after 25, 50, 100, 150, 200, and 300 ALE cycles using O_3 and HF as the reactants at 250 °C. The film thickness versus the number of ALE cycles is linear. An etch rate of 0.19 Å/cycle was obtained from the SE measurements using a least-squares fitting. The XRR measure-

DOI: 10.1021/acs.chemmater.7b02286
Chem. Mater. 2017, 29, 8202−8210

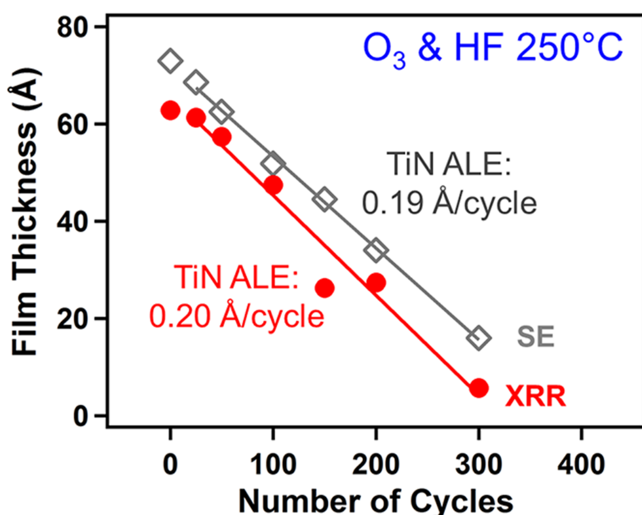

Figure 3. X-ray reflectivity and spectroscopic ellipsometry measurements of TiN film thickness versus number of O_3 and HF reaction cycles at 250 °C.

ments on the same samples yielded an etch rate of 0.20 Å/cycle. These XRR results are consistent with the SE results.

No TiN etch was observed when using O_2 by itself as the oxidation reactant together with HF. The oxidation reaction $TiN(s) + {}^3/_2O_2(g) \rightarrow TiO_2(s) + NO(g)$ is thermochemically favorable having a standard free energy change of $\Delta G° = -113.7$ kcal at 250 °C.[21] However, the oxidation of TiN by O_2 at <350 °C is known to slowly form a thin TiO_2 layer.[30,31] The surface of TiN also reacts with O_2 and creates an intermediate titanium oxynitride (TiO_xN_y) phase, in addition to a thin TiO_2 layer. The oxidation state of Ti in this intermediate phase is 3+ and 4+ by XPS analysis.[30] The strong oxidizing ability of O_3 may be necessary for the oxidation of TiN or TiO_xN_y to TiO_2. The TiO_2 layer can then be etched by HF during TiN ALE at 250 °C.

Figure 4 shows the self-limiting behavior for the O_3 and HF exposures during TiN ALE at 250 °C. The etch rates were obtained versus reactant exposure time while holding the other reactant exposure time constant. The etch rate was determined using the average thickness change during 200 ALE cycles. Figure 4a examines the self-limiting reaction using different O_3 exposure times with a HF exposure time of 1 s. A N_2 purge time of 30 s was used between reactant exposures. The etch rate increases and levels off at ~0.2 Å/cycle versus the O_3 exposure time. The oxidation of the TiN substrate is believed to be self-limiting because of the formation of a TiO_2 passivation layer on the TiN substrate that acts as a diffusion barrier.[32]

Figure 4b examines the self-limiting reaction using different HF exposure times with an O_3 exposure time of 3 s. The etch rate versus the HF exposure time increases and levels off at ~0.2 Å/cycle. The fluorination reaction is self-limiting because the etching reaction to produce volatile TiF_4 and H_2O is limited by the thickness of the TiO_2 layer on the TiN substrate. HF does not etch the TiN film by itself. Figure 2 shows that an HF exposure of 1 s is able to remove 25 ng/cm^2 or 0.66 Å of a TiO_2 film at 250 °C. This thickness of TiO_2 film removed by the HF exposure is much greater than the etch rate of 0.2 Å/cycle for the TiO_2 layer on the TiN substrate.

Figure 5 shows results for TiN ALE in the presence of various materials. These results demonstrate the selective etching of TiN using O_3 and HF as the reactants at 250 °C.

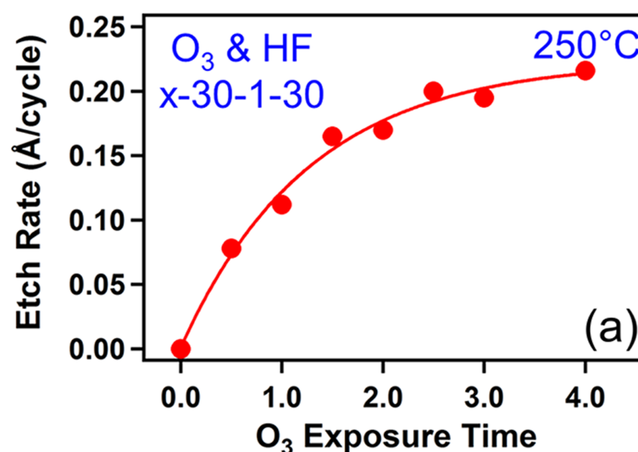

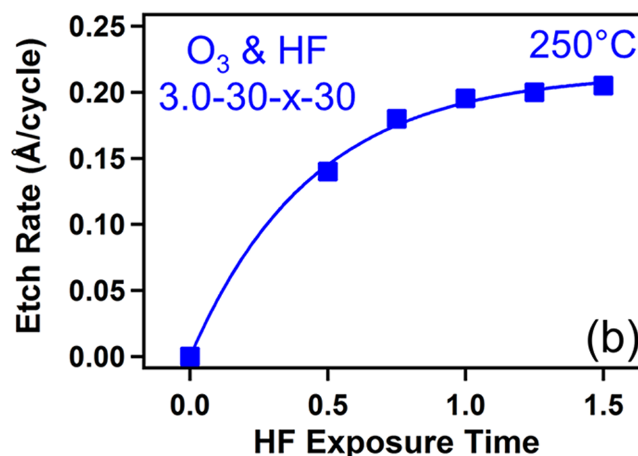

Figure 4. (a) Etch rates for TiN versus O_3 exposure time with constant HF exposure time of 1.0 s. (b) Etch rates for TiN versus HF exposure time with constant O_3 exposure time of 3.0 s.

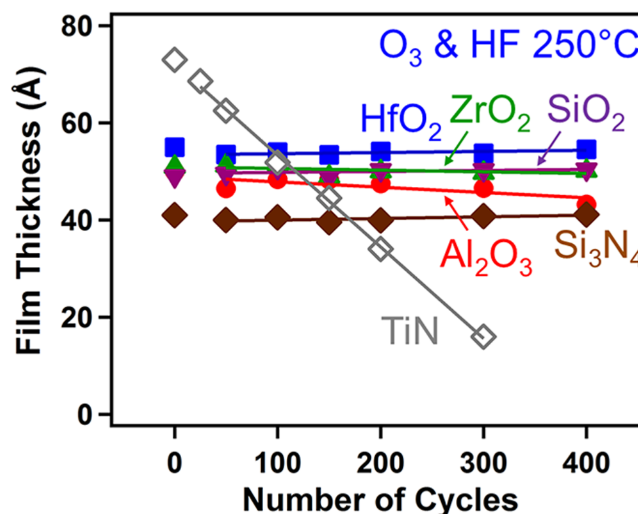

Figure 5. Film thickness versus number of O_3 and HF reaction cycles at 250 °C for Al_2O_3, HfO_2, ZrO_2, SiO_2, Si_3N_4, and TiN.

There are negligible thickness changes for Al_2O_3, HfO_2, ZrO_2, SiO_2, and Si_3N_4 during the TiN ALE reactions. The O_3 and HF exposures could not etch the Al_2O_3, HfO_2, and ZrO_2 metal oxides because the fluorides of these metal oxides, AlF_3, HfF_4, and ZrF_4, are stable and nonvolatile. The O_3 and HF exposures

DOI: 10.1021/acs.chemmater.7b02286
Chem. Mater. 2017, 29, 8202−8210

could also not etch silicon oxide and silicon nitride. In the absence of H_2O, dry HF can not etch SiO_2.[33] Previous thermal ALE studies using fluorination and ligand-exchange reactions could also not etch SiO_2 or Si_3N_4.[15] New approaches are needed for SiO_2 ALE and Si_3N_4 ALE.[16,18]

Figure 6 shows XRR scans for the initial TiN film on the Si wafer and for TiN films after various numbers of ALE cycles

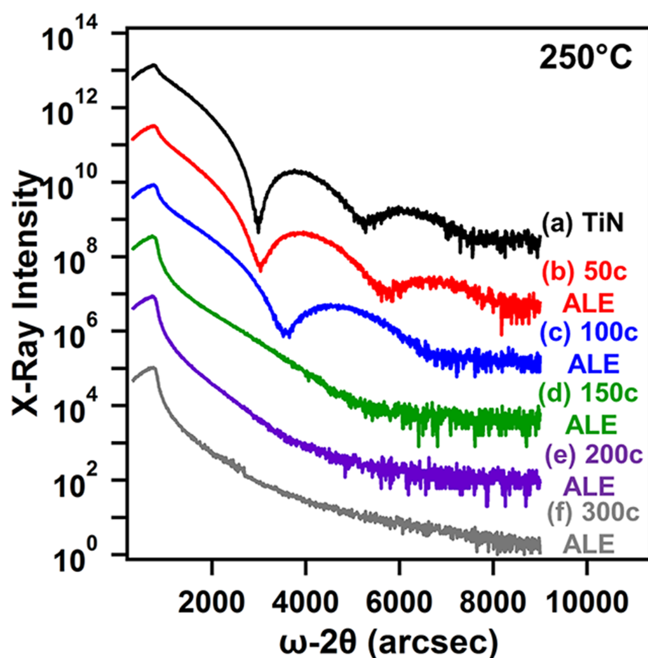

Figure 6. X-ray reflectivity scans versus number of O_3 and HF reaction cycles on TiN films at 250 °C.

with O_3 and HF as the reactants at 250 °C. The initial TiN film thickness is reduced linearly after various numbers of ALE cycles as shown in Figure 3. The XRR scans also reveal the roughness of the TiN films versus the ALE cycles. The roughness of initial TiN film was 9.3 Å. The roughness was then reduced as the TiN film was smoothed by the ALE process. The etched TiN films have roughness values of 8.5, 8.2, and 7.5 Å after 25, 50, and 100 ALE cycles, respectively. This decreased roughness versus number of TiN ALE cycles is consistent with the surface smoothing observed by previous studies of Al_2O_3 and HfO_2 ALE using fluorination and ligand-exchange reactions.[8,11]

Figure 7 shows the TiN ALE etch rates obtained at different temperatures using O_3 and HF as the reactants. The etch rates were obtained by the average of the thickness change measured by SE after 200 ALE cycles. All ALE reactions used an optimized reaction sequence of 3-30-1-30. The etch rate is 0.060 Å/cycle at 150 °C and increases to 0.20 Å/cycle at 250 °C. The etch rates are then constant with temperature between 250 and 350 °C. This result may indicate that a similar thickness for the TiO_2 layer is formed by O_3 and removed by HF at 250−350 °C. The HF can only remove the amount of TiO_2 that is formed during the O_3 exposure. This constant etch rate over a range of temperatures is similar to the "ALD window" often observed for many ALD processes.[4]

O_3 decomposition at high temperatures could affect the uniformity of the TiN film thicknesses in the reactor.[34] For exploration of this issue, studies were performed using 200 ALE cycles at 250, 300, and 350 °C where the etch rate was nearly

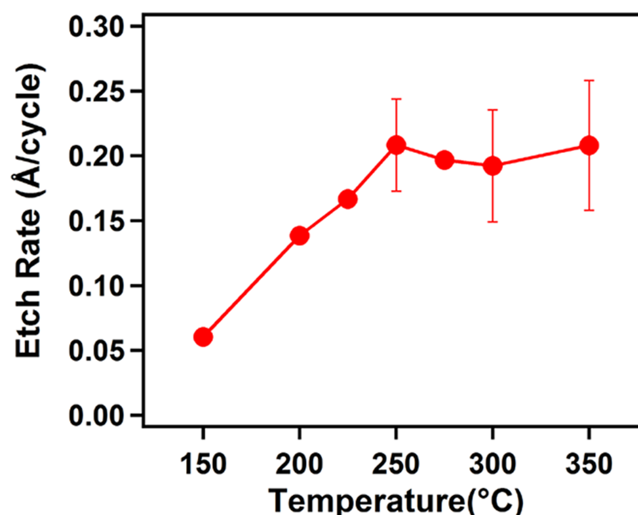

Figure 7. Etch rates for TiN ALE versus temperature using O_3 and HF as the reactants.

constant according to the results in Figure 7. Five TiN film samples were placed within a length of 12.7 cm in the hot-wall reactor as shown in Figure 8. The TiN thicknesses were measured before and after the 200 ALE cycles to determine the uniformity of the TiN film.

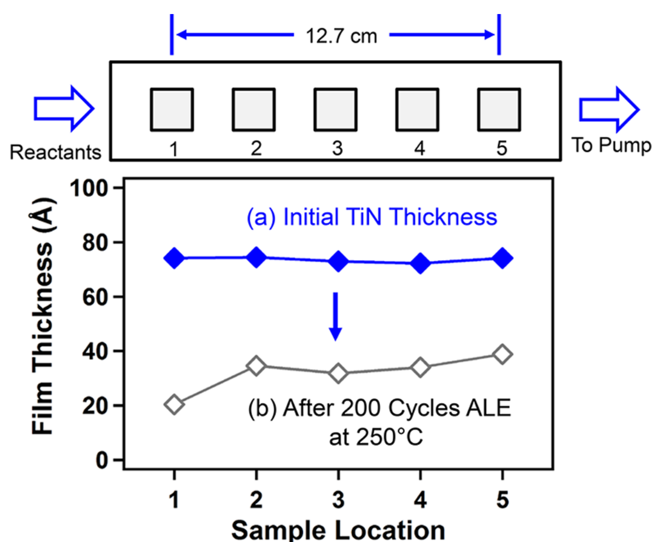

Figure 8. Film thickness for (a) initial TiN film and (b) after 200 TiN ALE cycles at 250 °C for different locations in the reactor.

Figure 8 reveals that TiN ALE yielded fairly uniform TiN film thicknesses after 200 ALE cycles at 250 °C. Positions 2−5 yield an etch rate of 0.19 Å/cycle. In contrast, a slightly larger etch rate of 0.27 Å/cycle is observed in Position 1 close to the reactant entry into the hot-wall reactor. This slightly larger etch rate may correspond with larger reactant exposures at Position 1.

Figure 9 shows uniformity results obtained at a higher temperature of 350 °C. These film thicknesses after 200 ALE cycles indicate that a lower etch rate is observed at the downstream positions. These downstream positions are furthest from the reactant entry into the hot-wall reactor. The recombination between gaseous O_3 molecules is negligible at a reaction pressure of ∼1 Torr.[35] Consequently, this result

DOI: 10.1021/acs.chemmater.7b02286
Chem. Mater. 2017, 29, 8202−8210

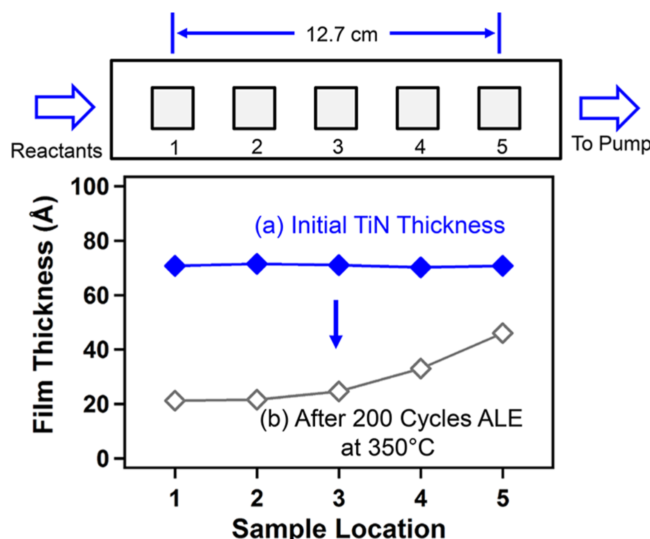

Figure 9. Film thickness for (a) initial TiN film and (b) after 200 TiN ALE cycles at 350 °C for different locations in the reactor.

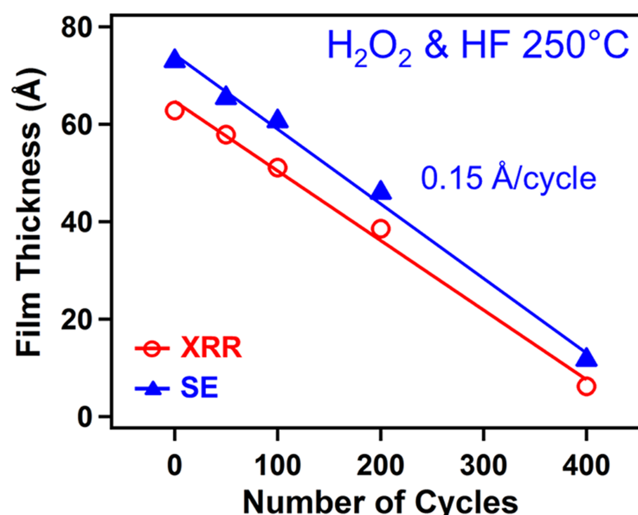

Figure 10. X-ray reflectivity and spectroscopic ellipsometry measurements of TiN film thickness versus number of H_2O_2 and HF reaction cycles at 250 °C.

may indicate that O_3 is undergoing some decomposition on the surfaces of the hot-wall reactor.

The decomposition of O_3 may be accelerated at the high temperature of 350 °C. This decomposition may lead to lower O_3 concentrations downstream in the reactor. These lower O_3 concentrations then produce lower TiN etch rates and thicker TiN film thicknesses. Similar effects were observed for ZnO ALD as a function of position in the reactor using $Zn(CH_2CH_3)_2$ and O_3 as the reactants.[25] Thinner ZnO ALD films were observed downstream in the reactor at 200 °C because of the lower O_3 concentrations.[25]

C. Thermal TiN ALE Using H_2O_2 and HF. Other oxidants, in addition to O_3, may be able to oxidize the TiN substrate and form a TiO_2 layer. H_2O_2 is a strong oxidizer that has been used as a reactant for metal oxide ALD.[26] H_2O_2/H_2O vapor derived from 30 to 50 wt % H_2O_2 solution has been used for ALD. H_2O_2 is a stronger oxidizer than O_2, but weaker than O_3. The redox potential of oxidants measured in solution is consistent with this order of oxidant strength.[36]

The proposed oxidation reaction of TiN using H_2O_2 can be expressed as

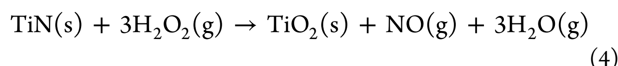

$$TiN(s) + 3H_2O_2(g) \rightarrow TiO_2(s) + NO(g) + 3H_2O(g) \quad (4)$$

This oxidation reaction is thermochemically favorable. The standard free energy is $\Delta G° = -211.6$ kcal/mol at 250 °C.[21]

Figure 10 shows the SE and XRR measurements of the initial TiN film thickness and the TiN film thickness after 50, 100, 200, and 400 ALE cycles using H_2O_2 and HF as the reactants at 250 °C. The film thickness versus the number of ALE cycles is linear. An etch rate of 0.15 Å/cycle was obtained by SE using a least-squares fitting. The XRR measurements on the same samples yielded an etch rate of 0.14 Å/cycle that is consistent with the SE results.

The ALE reactions using H_2O_2 and HF were also self-limiting. However, achieving reproducible results was challenging because of changes in the H_2O_2 concentration. Purging the excess H_2O after the H_2O_2/H_2O exposure was also difficult. There also may be a thermal decomposition of H_2O_2 at high temperatures. These factors contributed to making H_2O_2 more problematic than O_3 as an oxidant for TiN ALE.

Figure 11 shows the XRR scans of the initial TiN film on the Si wafer and the TiN films after various numbers of ALE cycles

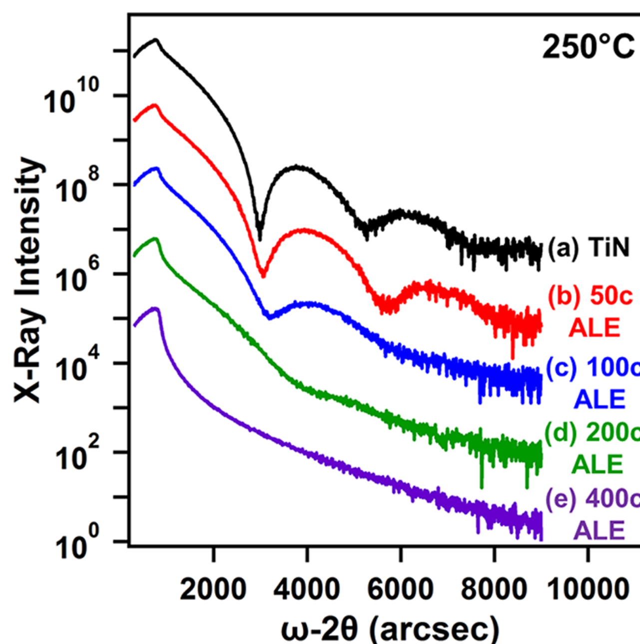

Figure 11. X-ray reflectivity scans versus number of H_2O_2 and HF reaction cycles on TiN films at 250 °C.

using H_2O_2 and HF as the reactants at 250 °C. The initial TiN film thickness of 63 Å was reduced versus number of ALE cycles as shown in Figure 10. The initial TiN film roughness was 9.3 Å. This roughness was reduced to 8.1 Å after 50 cycles and 6.5 Å after 100 ALE cycles. These measurements indicate that the TiN films were smoothed by TiN ALE using H_2O_2 and HF as the reactants. These results are consistent with the TiN film smoothing obtained from Figure 6 during TiN ALE using O_3 and HF as the reactants.

D. Generality of Thermal ALE Using Oxidation and Fluorination Reactions. The ALE of other materials including metal nitrides, metal sulfides, metal selenides, and

DOI: 10.1021/acs.chemmater.7b02286
Chem. Mater. 2017, 29, 8202−8210

elemental metals should be possible using sequential, self-limiting oxidation and fluorination reactions. This approach requires that oxidation by oxidants, such as O_3 and H_2O_2, is able to form a self-passivating metal oxide layer with a finite thickness that prevents further oxidation. The fluorination reactants, such as HF and SF_4, then remove only the metal oxide layer formed during the oxidation step. The removal occurs because the fluorides produced by the fluorination reactions are volatile. The oxygen in the metal oxide is removed as H_2O and SO_2 by HF and SF_4, respectively.

ALE processes using oxidation and fluorination reactions for representative materials are given in Table 1. The oxidation

Table 1. ALE Using Oxidation and Fluorination Reactions for Various Materials[a]

Metal Nitride
oxidation: $TiN + 3O_3 \rightarrow TiO_2 + NO + 3O_2$ ($\Delta G° = -241$ kcal/mol)
fluorination: $TiO_2 + SF_4 \rightarrow TiF_4 + SO_2$ ($\Delta G° = -62$ kcal/mol)
overall: $TiN + 3O_3 + SF_4 \rightarrow TiF_4 + NO + 3O_2 + SO_2$
Metal Carbide
oxidation: $NbC + {}^7/_2O_3 \rightarrow {}^1/_2Nb_2O_5 + CO + {}^7/_2O_2$ ($\Delta G° = -353$ kcal/mol)
fluorination: ${}^1/_2Nb_2O_5 + {}^5/_4SF_4 \rightarrow NbF_5 + {}^5/_4SO_2$ ($\Delta G° = -74$ kcal/mol)
overall: $NbC + {}^7/_2O_3 + {}^5/_4SF_4 \rightarrow NbF_5 + CO + {}^7/_2O_2 + {}^5/_4SO_2$
Metal Sulfide
oxidation: $WS_2 + 7O_3 \rightarrow WO_3 + 2SO_2 + 7O_2$ ($\Delta G° = -552$ kcal/mol)
fluorination: $WO_3 + {}^3/_2SF_4 \rightarrow WF_6 + {}^3/_2SO_2$ ($\Delta G° = -68$ kcal/mol)
overall: $WS_2 + 7O_3 + {}^3/_2SF_4 \rightarrow WF_6 + {}^7/_2SO_2 + 7O_2$
Metal Selenide
oxidation: $MoSe_2 + 9O_3 \rightarrow MoO_3 + 2SeO_3 + 9O_2$ ($\Delta G° = -519$ kcal/mol)
fluorination: $MoO_3 + {}^3/_2SF_4 \rightarrow MoF_6 + {}^3/_2SO_2$ ($\Delta G° = -43$ kcal/mol)
overall: $MoSe_2 + 9O_3 + {}^3/_2SF_4 \rightarrow MoF_6 + 2SeO_3 + 9O_2 + {}^3/_2SO_2$
Elemental Metal
oxidation: $Ta + {}^5/_2O_3 \rightarrow {}^1/_2Ta_2O_5 + {}^5/_2O_2$ ($\Delta G° = -323$ kcal/mol)
fluorination: ${}^1/_2Ta_2O_5 + {}^5/_4SF_4 \rightarrow TaF_5 + {}^5/_4SO_2$ ($\Delta G° = -79$ kcal/mol)
overall: $Ta + {}^5/_2O_3 + {}^5/_4SF_4 \rightarrow TaF_5 + {}^5/_2O_2 + {}^5/_4SO_2$

[a]Standard free energy change values are given at 250 °C.[21]

reactions for many transition metal nitrides that have volatile metal fluorides, such as TiN, to form their corresponding metal oxides are very favorable. The $\Delta G°$ values for the oxidation of TiN, TaN, NbN, VN, W_2N, Mo_2N, MoN, and CrN using O_3 to form TiO_2, Ta_2O_5, Nb_2O_5, V_2O_5, WO_3, MoO_3, MoO_3, and CrO_3 are −241, −296, −284, −246, −294, −280, −298, and −238 kcal/mol at 250 °C, respectively.[21] The $\Delta G°$ values for oxidation using H_2O_2 are somewhat lower, but still very favorable, with $\Delta G°$ values <−200 kcal/mol.[21]

The fluorinations of these metal oxides should all yield volatile metal fluorides. The $\Delta G°$ values for the fluorination of TiO_2, Ta_2O_5, Nb_2O_5, V_2O_5, WO_3, MoO_3, and CrO_3 using SF_4 to form TiF_4, TaF_5, NbF_5, VF_5, WF_6, MoF_6, and CrF_6 are −62, −79, −74, −45, −68, −53, and −40 kcal/mol at 250 °C, respectively.[21] These metal fluorides are all volatile. For other metal nitrides that do not produce volatile fluorides after the fluorination of the metal oxide, a ligand-exchange reaction may be required to remove the metal fluoride.[10]

Metal carbides are important materials that can be used as gate electrode materials with low work functions in semiconductor devices.[37] Metal carbides have many similar properties to metal nitrides such as structure, bonding characteristics, and electronic properties.[38] The oxidation reactions for transition metal carbides to form their corresponding metal oxides are very favorable. The $\Delta G°$ values for the oxidation of TaC, VC, and W_2C using O_3 to form Ta_2O_5, V_2O_5, and WO_3 are −369, −321, and −334 kcal/mol at 250 °C, respectively.[21] These reactions assume CO as an etching product. The Ta_2O_5, V_2O_5, and WO_3 metal oxides then should produce volatile fluorides during the fluorination reaction using HF or SF_4.

Transition metal sulfides and selenides are important 2D semiconductor materials.[39] The oxidation of metal sulfides and selenides to form their corresponding metal oxides is also favorable. The $\Delta G°$ values for the oxidation of WS_2, MoS_2, WSe_2, and $MoSe_2$ using O_3 to form WO_3, MoO_3, WO_3, and MoO_3 are −553, −526, −531, and −515 kcal/mol at 250 °C, respectively.[21] The oxidation should also yield volatile SO_2 or SeO_3 reaction products. In addition to these thermochemical calculations, previous studies have recently reported the oxidation of WSe_2 to form a WO_x layer on WSe_2.[40,41] These metal oxides should then form volatile metal fluorides after fluorination with SF_4.

Elemental metals with volatile metal fluorides can also be etched using oxidation and fluorination reactions. The $\Delta G°$ values for the oxidation of Ti, Ta, Nb, V, W, Mo, and Cr using O_3 to form TiO_2, Ta_2O_5, Nb_2O_5, V_2O_5, WO_3, MoO_3, and CrO_3 are −288, −323, −305, −264, −296, −273, and −234 kcal/mol at 250 °C, respectively.[21] The oxidation reaction is expected to form a self-passivating metal oxide on the surface of the metal.[32] If the oxide layer does not self-limit versus oxidant exposure, other milder oxidation reactants such as NO_2,[42] N_2O,[43] and NO[44] may be useful to obtain a self-limiting oxide thickness. These metal oxides should then form volatile metal fluorides after fluorination with HF or SF_4.

The choice of the fluorination reactant is important for metal ALE using oxidation and fluorination reactions. Some metals will spontaneously etch with fluorination reactants that are stronger than HF. For example, XeF_2 and F_2 are both strong fluorination reagents. After removing the metal oxide, XeF_2 and F_2 could proceed to etch the underlying metal spontaneously. For example, XeF_2 spontaneously etches Ti, V, Nb, Ta, Mo, W, and metal alloys such as Ti/W.[45] In contrast, HF can often etch the metal oxide layer without etching the underlying metal.

Some metals will also be difficult to etch using oxidation and fluorination reactions because their metal oxides are not favorable or stable. For example, Re and Pt have volatile fluorides such as ReF_6 and PtF_6, respectively. Re ALE may be difficult because the thermochemistry for fluorination of ReO_3 is not very favorable. The reaction $ReO_3(s) + {}^3/_2SF_4(g) \rightarrow ReF_6(g) + {}^3/_2SO_2(g)$ has a $\Delta G°$ value of +9 kcal/mol at 250 °C and becomes negative at >450 °C.[21] Pt ALE may also be difficult because PtO_3 is not a stable oxide. The formation of PtO_2 on Pt may be possible, but PtF_4 is not volatile.[46]

IV. CONCLUSIONS

Thermal ALE of TiN can be accomplished using sequential oxidation and fluorination reactions that yield volatile metal fluorides. This work employed two oxidation reagents, O_3 and H_2O_2, for the oxidation reaction. HF derived from HF-pyridine solution was then used for the fluorination reaction. TiN ALE occurred with a linear reduction of the TiN film thickness versus the number of ALE cycles. The etch rate of TiN ALE versus temperature using O_3 and HF as the reactants increased from 0.06 Å/cycle at 150 °C to 0.20 Å/cycle at 250 °C. The etch rate was then constant at ≥250 °C.

The selective etching of TiN was also observed in the presence of other materials using O_3 and HF as the reactants.

DOI: 10.1021/acs.chemmater.7b02286
Chem. Mater. 2017, 29, 8202−8210

TiN ALE occurred selectively with no observed etching of the Al_2O_3, HfO_2, ZrO_2, SiO_2, and Si_3N_4 surrounding materials. TiN ALE was also achieved using H_2O_2 and HF as the reactants. An etch rate of 0.15 Å/cycle was measured at 250 °C. TiN ALE led to surface smoothing when using either O_3 or H_2O_2 as the oxidation reactant.

The overall etching reaction is believed to follow the following reaction: $TiN + 3O_3 + 4HF \rightarrow TiF_4 + NO + 3O_2 + 2H_2O$. In the proposed reaction mechanism, the oxidizing reactant, O_3, oxidizes TiN and forms a TiO_2 layer on the TiN substrate. The HF exposure then removes the TiO_2 layer by producing volatile TiF_4 and H_2O from TiO_2. The ALE of many other metal nitrides should be possible using the oxidation and fluorination reactions that yield a volatile metal fluoride. This ALE reaction mechanism should also be applicable for the ALE of metal carbides, metal sulfides, metal selenides, and elemental metals.

■ AUTHOR INFORMATION

ORCID

Younghee Lee: 0000-0002-0492-6826

Steven M. George: 0000-0003-0253-9184

Notes

The authors declare no competing financial interest.

■ ACKNOWLEDGMENTS

This research was funded by Intel Corporation through a Member Specific Research Project administered by the Semiconductor Research Corporation. The authors would like to acknowledge SEMATECH for providing various thin films on silicon wafers.

■ REFERENCES

(1) Kanarik, K. J.; Lill, T.; Hudson, E. A.; Sriraman, S.; Tan, S.; Marks, J.; Vahedi, V.; Gottscho, R. A. Overview of Atomic Layer Etching in the Semiconductor Industry. *J. Vac. Sci. Technol., A* **2015**, *33*, 020802.

(2) Lill, T.; Kanarik, K. J.; Tan, S.; Shen, M.; Hudson, E.; Pan, Y.; Marks, J.; Vahedi, V.; Gottscho, R. A. Directional Atomic Layer Etching. *Encyclopedia of Plasma Technology* **2016**, 133.

(3) Faraz, T.; Roozeboom, F.; Knoops, H. C. M.; Kessels, W. M. M. Atomic Layer Etching: What Can We Learn from Atomic Layer Deposition? *ECS J. Solid State Sci. Technol.* **2015**, *4*, N5023−N5032.

(4) George, S. M. Atomic Layer Deposition: An Overview. *Chem. Rev.* **2010**, *110*, 111−131.

(5) Oehrlein, G. S.; Metzler, D.; Li, C. Atomic Layer Etching at the Tipping Point: An Overview. *ECS J. Solid State Sci. Technol.* **2015**, *4*, N5041−N5053.

(6) Agarwal, A.; Kushner, M. J. Plasma Atomic Layer Etching Using Conventional Plasma Equipment. *J. Vac. Sci. Technol., A* **2009**, *27*, 37−50.

(7) George, S. M.; Lee, Y. Prospects for Thermal Atomic Layer Etching Using Sequential, Self-Limiting Fluorination and Ligand-Exchange Reactions. *ACS Nano* **2016**, *10*, 4889−4894.

(8) Lee, Y.; George, S. M. Atomic Layer Etching of Al_2O_3 Using Sequential, Self-Limiting Thermal Reactions with $Sn(acac)_2$ and HF. *ACS Nano* **2015**, *9*, 2061−2070.

(9) Osakada, K., Transmetalation. In *Fundamentals of Molecular Catalysis, Current Methods in Inorganic Chemistry*, Vol. 3; Kurosawa, H., Yamamoto, A., Eds.; Elsevier Science: Amsterdam, 2003.

(10) Johnson, N. R.; Sun, H.; Sharma, K.; George, S. M. Thermal Atomic Layer Etching of Crystalline Aluminum Nitride Using Sequential, Self-Limiting Hydrogen Fluoride and $Sn(acac)_2$ Reactions and Enhancement by H_2 and Ar Plasmas. *J. Vac. Sci. Technol., A* **2016**, *34*, 050603.

(11) Lee, Y.; DuMont, J. W.; George, S. M. Atomic Layer Etching of HfO_2 Using Sequential, Self-Limiting Thermal Reactions with $Sn(acac)_2$ and HF. *ECS J. Solid State Sci. Technol.* **2015**, *4*, N5013−N5022.

(12) Lee, Y.; DuMont, J. W.; George, S. M. Atomic Layer Etching of AlF_3 Using Sequential, Self-Limiting Thermal Reactions with $Sn(acac)_2$ and Hydrogen Fluoride. *J. Phys. Chem. C* **2015**, *119*, 25385−25393.

(13) Lee, Y.; DuMont, J. W.; George, S. M. Mechanism of Thermal Al_2O_3 Atomic Layer Etching Using Sequential Reactions with $Sn(acac)_2$ and HF. *Chem. Mater.* **2015**, *27*, 3648−3657.

(14) Lee, Y.; DuMont, J. W.; George, S. M. Trimethylaluminum as the Metal Precursor for the Atomic Layer Etching of Al_2O_3 Using Sequential, Self-Limiting Thermal Reactions. *Chem. Mater.* **2016**, *28*, 2994−3003.

(15) Lee, Y.; Huffman, C.; George, S. M. Selectivity in Thermal Atomic Layer Etching Using Sequential, Self-Limiting Fluorination and Ligand-Exchange Reactions. *Chem. Mater.* **2016**, *28*, 7657−7665.

(16) Zywotko, D. R.; George, S. M. Thermal Atomic Layer Etching of ZnO by a "Conversion-Etch" Mechanism Using Sequential Exposures of Hydrogen Fluoride and Trimethylaluminum. *Chem. Mater.* **2017**, *29*, 1183−1191.

(17) DuMont, J. W.; George, S. M. Competition Between Al_2O_3 Atomic Layer Etching and AlF_3 Atomic Layer Deposition Using Sequential Exposures of Trimethylaluminum and Hydrogen Fluoride. *J. Chem. Phys.* **2017**, *146*, 052819.

(18) DuMont, J. W.; Marquardt, A. E.; Cano, A. M.; George, S. M. Thermal Atomic Layer Etching of SiO_2 by a "Conversion-Etch" Mechanism Using Sequential Reactions of Trimethylaluminum and Hydrogen Fluoride. *ACS Appl. Mater. Interfaces* **2017**, *9*, 10296−10307.

(19) Kim, H. Atomic Layer Deposition of Metal and Nitride Thin Films: Current Research Efforts and Applications for Semiconductor Device Processing. *J. Vac. Sci. Technol., B: Microelectron. Process. Phenom.* **2003**, *21*, 2231−2261.

(20) Wittmer, M. Properties and Microelectronic Applications of Thin Films of Refractory Metal Nitrides. *J. Vac. Sci. Technol., A* **1985**, *3*, 1797−1803.

(21) *HSC Chemistry 5.1*; Outokumpu Research Oy: Pori, Finland.

(22) Elam, J. W.; Groner, M. D.; George, S. M. Viscous Flow Reactor with Quartz Crystal Microbalance for Thin Film Growth by Atomic Layer Deposition. *Rev. Sci. Instrum.* **2002**, *73*, 2981−2987.

(23) Ritala, M.; Leskela, M.; Nykanen, E.; Soininen, P.; Niinisto, L. Growth of Titanium Dioxide Thin Films by Atomic Layer Epitaxy. *Thin Solid Films* **1993**, *225*, 288−295.

(24) Lee, Y.; DuMont, J. W.; Cavanagh, A. S.; George, S. M. Atomic Layer Deposition of AlF_3 Using Trimethylaluminum and Hydrogen Fluoride. *J. Phys. Chem. C* **2015**, *119*, 14185−14194.

(25) Knoops, H. C. M.; Elam, J. W.; Libera, J. A.; Kessels, W. M. M. Surface Loss in Ozone-Based Atomic Layer Deposition Processes. *Chem. Mater.* **2011**, *23*, 2381−2387.

(26) Niinisto, L.; Paivasaari, J.; Niinisto, J.; Putkonen, M.; Nieminen, M. Advanced Electronic and Optoelectronic Materials by Atomic Layer Deposition: An Overview with Special Emphasis on Recent Progress in Processing of High-k Dielectrics and Other Oxide Materials. *Phys. Status Solidi A* **2004**, *201*, 1443−1452.

(27) Fink, C. K.; Nakamura, K.; Ichimura, S.; Jenkins, S. J. Silicon Oxidation by Ozone. *J. Phys.: Condens. Matter* **2009**, *21*, 183001.

(28) Kuznetsova, A.; Yates, J. T.; Zhou, G.; Yang, J. C.; Chen, X. D. Making a Superior Oxide Corrosion Passivation Layer on Aluminum Using Ozone. *Langmuir* **2001**, *17*, 2146−2152.

(29) Haynes, W. M., Ed. *CRC Handbook of Chemistry and Physics*, 96th ed.; CRC Press, LLC: Boca Raton, FL, 2015.

(30) Glaser, A.; Surnev, S.; Netzer, F. P.; Fateh, N.; Fontalvo, G. A.; Mitterer, C. Oxidation of Vanadium Nitride and Titanium Nitride Coatings. *Surf. Sci.* **2007**, *601*, 1153−1159.

(31) Saha, N. C.; Tompkins, H. G. Titanium Nitride Oxidation Chemistry - An X-Ray Photoelectron Spectroscopy Study. *J. Appl. Phys.* **1992**, *72*, 3072−3079.

DOI: 10.1021/acs.chemmater.7b02286
Chem. Mater. 2017, 29, 8202−8210

(32) Deal, B. E.; Grove, A. S. General Relationship for Thermal Oxidation of Silicon. *J. Appl. Phys.* **1965**, *36*, 3770−3778.
(33) Helms, C. R.; Deal, B. E. Mechanisms of the HF/H_2O Vapor Phase Etching of SiO_2. *J. Vac. Sci. Technol., A* **1992**, *10*, 806−811.
(34) Benson, S. W.; Axworthy, A. E. Mechanism of the Gas Phase, Thermal Decomposition of Ozone. *J. Chem. Phys.* **1957**, *26*, 1718−1726.
(35) Itoh, H.; Rusinov, I. M.; Suzuki, S.; Suzuki, T. Variation of Ozone Reflection Coefficient at a Metal Surface with its Gradual Oxidation. *Plasma Processes Polym.* **2005**, *2*, 227−231.
(36) Oyama, S. T. Chemical and Catalytic Properties of Ozone. *Catal. Rev.: Sci. Eng.* **2000**, *42*, 279−322.
(37) Hwang, W. S.; Chan, D. S. H.; Cho, B. J. Metal Carbides for Band-Edge Work Function Metal Gate CMOS Devices. *IEEE Trans. Electron Devices* **2008**, *55*, 2469−2474.
(38) Toth, L. E.; *Transition Metal Carbides and Nitrides*; Academic Press: New York, 1971.
(39) Chhowalla, M.; Shin, H. S.; Eda, G.; Li, L. J.; Loh, K. P.; Zhang, H. The Chemistry of Two-Dimensional Layered Transition Metal Dichalcogenide Nanosheets,. *Nat. Chem.* **2013**, *5*, 263−275.
(40) Yamamoto, M.; Dutta, S.; Aikawa, S.; Nakaharai, S.; Wakabayashi, K.; Fuhrer, M. S.; Ueno, K.; Tsukagoshi, K. Self-Limiting Layer-by-Layer Oxidation of Atomically Thin WSe_2. *Nano Lett.* **2015**, *15*, 2067−2073.
(41) Yamamoto, M.; Nakaharai, S.; Ueno, K.; Tsukagoshi, K. Self-Limiting Oxides on WSe_2 as Controlled Surface Acceptors and Low-Resistance Hole Contacts. *Nano Lett.* **2016**, *16*, 2720−2727.
(42) Drozd, V. E.; Baraban, A. P.; Nikiforova, I. O. Electrical Properties of Si-Al_2O_3 Structures grown by ML-ALE. *Appl. Surf. Sci.* **1994**, *82*−*83*, 583−586.
(43) Kumagai, H.; Toyoda, K.; Matsumoto, M.; Obara, M. Comparative Study of Al_2O_3 Optical Crystalline Thin Films Grown by Vapor Combinations of $Al(CH_3)_3/N_2O$ and $Al(CH_3)_3/H_2O_2$. *Jpn. J. Appl. Phys., Part 1* **1993**, *32*, 6137−6140.
(44) Heo, J.; Kim, S. B.; Gordon, R. G. Atomic Layer Deposition of Tin Oxide with Nitric Oxide as an Oxidant Gas. *J. Mater. Chem.* **2012**, *22*, 4599−4602.
(45) Williams, K. R.; Gupta, K.; Wasilik, M. Etch Rates for Micromachining Processing - Part II. *J. Microelectromech. Syst.* **2003**, *12*, 761−778.
(46) Ellinger, C.; Stierle, A.; Robinson, I. K.; Nefedov, A.; Dosch, H. Atmospheric Pressure Oxidation of Pt(111). *J. Phys.: Condens. Matter* **2008**, *20*, 184013.

DOI: 10.1021/acs.chemmater.7b02286
Chem. Mater. 2017, 29, 8202−8210